CrossMark

Adsorption of uranium (VI) onto amidoxime-functionalized ultra-high molecular weight polyethylene fibers from aqueous solution

Chun-Yu Xie[1,2] · Shi-Pei Jing[1] · Yu Wang[1] · Xiao Lin[1] · Hong-Liang Bao[1] ·
Cheng-Zhi Guan[1,2] · Chan Jin[1] · Jian-Qiang Wang[1,2]

Abstract Amidoxime-functionalized ultra-high molecular weight polyethylene fibers (UHMWPEF-AO) were used to absorb uranium U(VI) from aqueous solutions. In this paper, we study effects of pH, initial U(VI) concentration, contact time, and temperature on U(VI) adsorption by UHMWPEF-AO. The adsorption process agrees well with pseudo-second-order and Langmuir model. UHMWPEF-AO exhibits excellent adsorptive performance for U(VI) with a maximum adsorption capacity of 176.12 mg/g at pH 4 and 298 K. The structures of UHMWPEF-AO and U(VI)-loaded UHMWPEF-AO are characterized by FT-IR and nano-CT. U(VI)-loaded UHMWPEF-AO is sintered after adsorption process to recycle absorbed U(VI). Powders collected after sintering process are examined by scanning electron microscopy and X-ray diffraction. These results indicate that UHMWPEF-AO is a promising candidate to remove U(VI) from uranium aqueous solutions.

Keywords Uranium · Adsorption · Kinetics · Isotherms · Sintering

✉ Jian-Qiang Wang
  wangjianqiang@sinap.ac.cn

1   Shanghai Institute of Applied Physics, Chinese Academy of Sciences, Shanghai 201800, China

2   University of Chinese Academy of Sciences, Beijing 100049, China

1 Introduction

Uranium concentration in the environment has been a public concern [1]. The maximum uranium concentration in drinking water is no more than 9, 20 and 20 μg/L, according to drinking water guidelines of the World Health Organization (WHO), Health Canada and Australian, respectively [2, 3]. Importantly, the inhalation of uranium and its compounds results in deposition in the lung and may further reach to the kidney through the blood steam, leading to progressive or irreversible kidney damage and failure, even death in acute cases [4–6]. The maximum daily intake of uranium issued by the WHO is 0.6 μg/kg of body weight daily [7]. Therefore, searching for appropriately effective techniques to adsorb uranium (VI) from aqueous solutions is of significance for both utilizing U(VI) and alleviating the environment problem.

Till now, numerous approaches, including ion-exchange, chemical precipitation, membrane dialysis, solvent extraction, and adsorption, have been studied extensively for U(VI) extraction [8, 9]. Among them, the adsorption method is prospective due to its reusability, cost effectiveness, ease of operation and low sludge production [10]. Developing high-performance adsorbent is of great importance for improving adsorptive effect. Researchers developed a variety of functionalized materials as adsorbents, such as magnetic composites [11–14], activated carbon [15], nanoporous carbons [16], graphene oxides [17]. In addition, amidoxime, an exceptional amphoteric group, is often chosen to modify different matrix materials on account of sorption rate, efficient U(VI) loading capacity, and environmental friendliness [18, 19].

In this study, amidoxime-functionalized ultra-high molecular weight polyethylene fibers (abbreviated to

UHMWPEF-AO) were used to absorb U(VI) from aqueous solutions. UHMWPEF-AO exhibits high mechanical properties and resistance to chemical corrosion and weathering. Furthermore, the raw material of the as-prepared samples, PE nonwoven fabrics or long fibers, is of easy-access and low-cost. Notably, the adsorbed U(VI) could be recycled through sintering samples collected after adsorption equilibrium was reached, avoiding secondary pollution in common acid elution procedures.

2 Experimental

2.1 Apparatus

Fourier-transformed infrared (FT-IR) spectra were recorded by a Nicolet 6700 infrared spectrophotometer with a Nicolet continuum FT-IR microscope at Beamline 01B1 of Shanghai Synchrotron Radiation Facility. Nano-computed tomography (Nano-CT) experiments were performed at Beamline BL01B of National Synchrotron Radiation Research Center (NSRRC). Samples for nano-CT were prepared by an FEI Helios NanoLab 600 Dual-Beam FIB-SEM (Focus Ion Beam Scanning Electron Microscopy). SEM images were acquired by Zeiss Merlin Compact LE0 1530 VP with an Inca X-Max energy-dispersive spectroscopy. X-ray diffraction (XRD) analysis was carried out on a Rigaku D/max-IIIB diffractometer using Cu Ka ray ($k = 1.54178$), with the X-ray source being operated at 40 kV and 150 mA.

2.2 Samples and reagents

UHMWPEF-AO synthesized by γ-irradiation-induced graft copolymerization and amidoximation [20] were provided by the radiation chemistry laboratory at Shanghai Institute of Applied Physics, Chinese Academy of Sciences. Different concentrations of U(VI) solution were prepared by diluting uranium standard solution of 1000 mg/L U(VI) concentration by distilled water to desired concentrations. Uranium standard solution, sodium hydroxide and hydrochloric acid were from Sinopharm Chemical Reagent Co., Ltd. All reagents were of AR grade and used without further purification.

2.3 Adsorption experiments

The effects of solution pH, contact time, initial concentration and temperature on adsorption of U(VI) were investigated. Typically, a certain amount of UHMWPEF-AO (5 mg) was added into 5 mL U(VI) solution in polyethylene tubes. HCl and NaOH solutions were used to adjust pH to expected values. After 24 h, the UHMWPEF-

AO samples were taken out with tweezers. The concentrations of U(VI) were measured by inductively coupled plasma atomic emission spectroscopy (Optima 8000, Perkin Elmer). The amount (mg/g) of adsorbed U(VI) was calculated by $q_e = (C_0 - C_e)V/m$, where C_0 and C_e are U(VI) concentrations (mg/L) in starting solution and equilibrium solution, respectively; V is the volume (L) of starting solution, and m is the mass (g) of UHMWPEF-AO.

3 Results and discussion

3.1 Effect of pH

To examine the pH effect on U(VI) adsorption, the amount of adsorbed U(VI) at pH 1–7 was measured. As shown in Fig. 1, the amount of U(VI) absorbed on UHMWPEF-AO significantly increased with pH value until pH 4, where it began to decrease, indicating that the solution pH had strong influence on adsorption of U(VI).

In highly acidic aqueous solutions (pH $\leq$ 2), amine groups were protonated and formed $-NH_3^+$. Fewer binding sites were available for U(VI) due to competition of H^+ [21]. Moreover, the great majority of U(VI) were present in the form of UO_2^{2+} (Fig. 2), and electrostatic repulsion depressed reaction between protonated UHMWPEF-AO and UO_2^{2+}. Therefore, very few U(VI) were absorbed. When pH varied from 2 to 4, concentration of OH^- increased and positively charged UHMWPEF-AO transformed to electrically neutral molecule. Meanwhile, some UO_2^{2+} ions were hydrolyzed to UO_2OH^+, which could form stable complexes with UHMWPEF-AO [22]. Consequently, adsorption of U(VI) increased and reached a maximum value (99.43 mg/g) at pH 4. When pH increased >4, further hydrolysis of U(VI) formed $UO_2(OH)_2 \cdot H_2O$ (a colloid deposit) and resulted in a decrease in adsorption
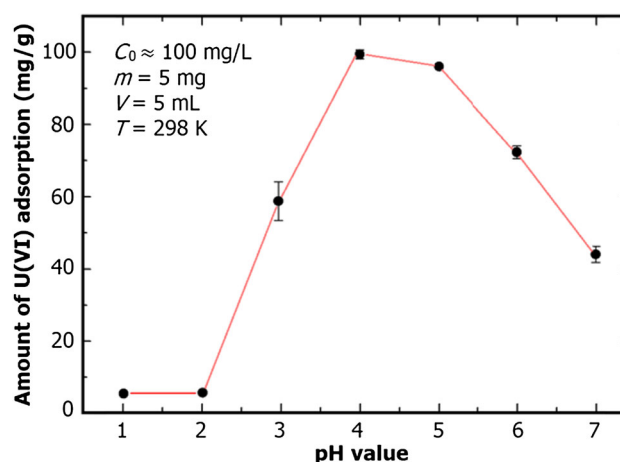
Fig. 1 (Color online) Effects of pH on adsorption of U(VI)
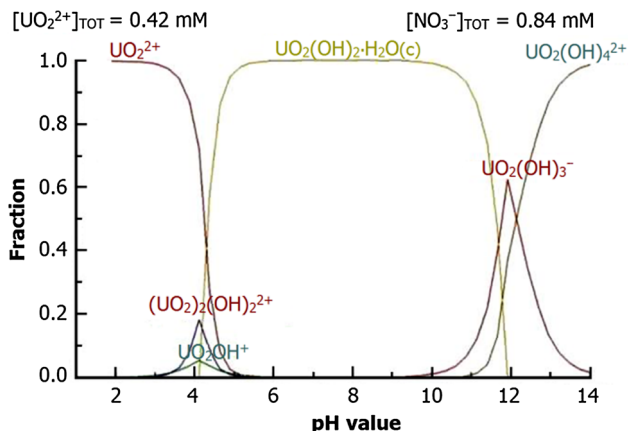
Fig. 2 (Color online) Distribution of U(VI) species in aqueous solution. Calculated by Medusa program (C(U) = 100 mg/L, pH 0–14)

capacity. Therefore, pH 4.0 was chosen for the following experiments.

3.2 Effect of contact time and kinetic studies

To investigate dynamic characteristics of adsorption process, experiments lasting different contacting time (5 min–24 h) were performed. As shown in Fig. 3, adsorption of U(VI) could be divided into two stages: U(VI) uptake increased sharply in the first 180 min, and around 78% of the adsorption was achieved in this stage. In the second stage, the adsorption slowed down and reached equilibrium finally. In further experiments, 24 h was selected to insure the equilibrium of U(VI) adsorption on UHMWPEF-AO.

The pseudo-first-order and pseudo-second-order models were used to analyze the acquired data. The former is based on adsorption capacity, while the latter assumes the rate-
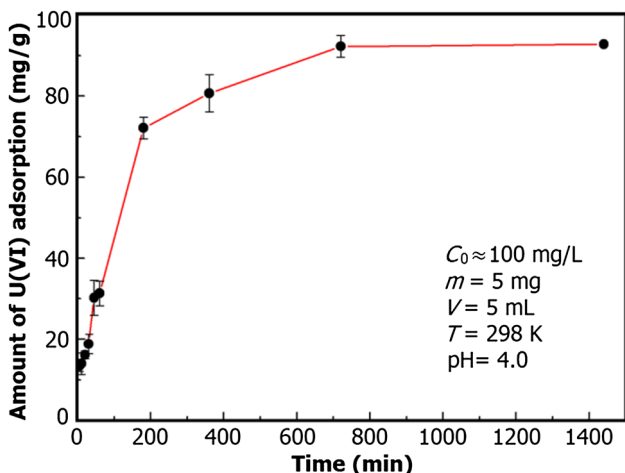
Fig. 3 (Color online) Effect of contact time on adsorption of U(VI)

determining step is a chemisorption process including valence forces through either sharing or the electron interchange between adsorbent and adsorbate [23]. The two models can be written as:

$$\ln(q_e - q_t) = \ln q_e - k_1 t, \tag{1}$$

$$\frac{t}{q_t} = \frac{1}{k_2 q_e^2} + \frac{t}{q_e}, \tag{2}$$

where q_e and q_t represent the amount of absorbed U(VI) at equilibrium time (min) and time t (min), respectively; and k_1 and k_2 are coefficients. The plots of $\ln(q_e - q_t)$ versus t, and t/q_t against t, are shown in Fig. 4. The values of k_1, k_2, q_e are given in Table 1. The higher correlation coefficient value of pseudo-second-order implied the second-order nature. This indicates that the dominant adsorption mechanism is chemisorption or strong surface complexation, instead of mass transport.

3.3 Effects of initial concentration and isotherm studies

Adsorption capacity depends in part on initial U(VI) concentration in the whole aqueous solution. At low concentrations, binding sites of UHMWPEF-AO are partially occupied by U(VI). With increasing concentration, fewer binding sites are available and the adsorption saturates finally. Experiments were carried out at different initial U(VI) concentrations (50–350 mg/L). The obtained adsorption isotherm of U(VI) on UHMWPEF-AO is shown in Fig. 5.

Langmuir and Freundlich isotherm models were applied to simulate the experimental data. Langmuir isotherm model assumes homogeneous monolayer adsorption. Freundlich isotherm model is widely used in heterogeneous systems [24]. They were expressed, respectively, as follows:

$$\frac{C_e}{q_e} = \frac{1}{b \cdot q_m} + \frac{C_e}{q_m}, \tag{3}$$

$$\ln q_e = \ln k + \frac{1}{n} \ln c_e, \tag{4}$$

where C_e (mg/L) and q_e (mg/g) are the U(VI) concentration in solutions and the amounts of absorbed U(VI) at equilibrium time, separately; q_m (mg/g) is the maximum adsorption capacity; b (L/mg) is Langmuir constant, k (L/g) and n are Freundlich constants associated with adsorption capacity and adsorption intensity, respectively. The plots of C_e/q_e versus C_e, and $\ln q_e$ against $\ln C_e$, are shown in Fig. 6. The values of b, q_m, k and n calculated from the intercepts and slopes in Fig. 6 are given in Table 2. The Langmuir model fits the data better, indicating a monolayer adsorption of $q_m = 176.99$ mg/g. In Table 3, the q_m of
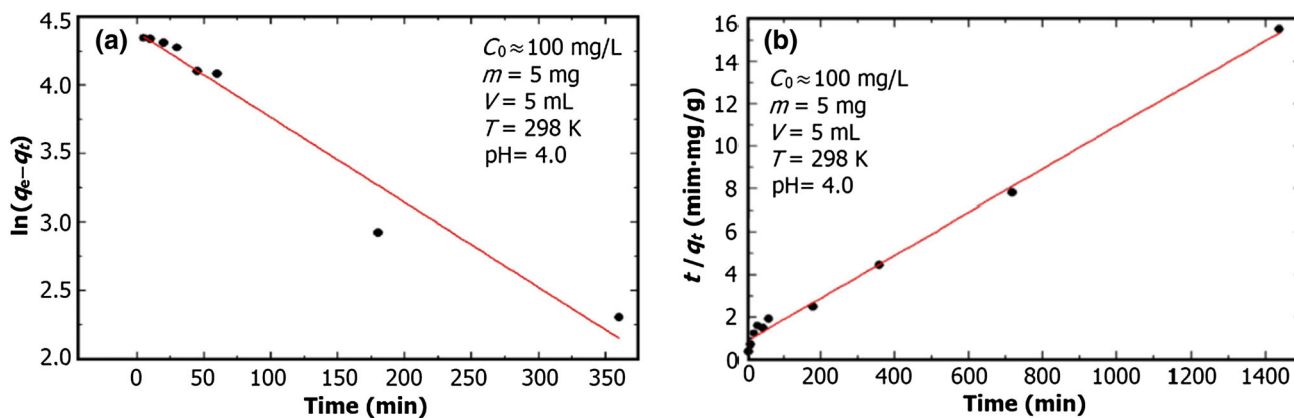
Fig. 4 (Color online) Pseudo-first-order (**a**) and pseudo-second-order (**b**) plots for the adsorption of U(VI) by UHMWPEF-AO

Table 1 Kinetic parameters of U(VI) adsorption on UHMWPEF-AO

Kinetic model	q_e^{cal} (mg/g)	k_1/k_2 (g/mg/min^2)	R^2
Pseudo-first order	90.72	0.0083	0.9772
Pseudo-second order	99.40	1.16×10^{-4}	0.9946

$T = 25$ °C, $C_0 = 100$ mg/L, $q_e^{exp} = 92.79$ mg/g
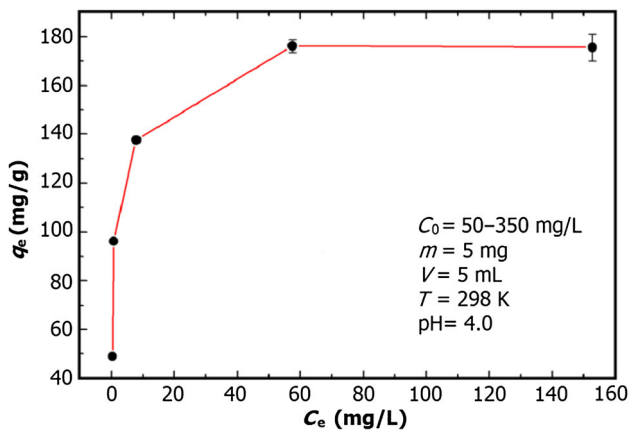
Fig. 5 (Color online) Absorbed U(VI) as a function of U(VI) concentrations in equilibrium solution, obtained at initial U(VI) concentrations of 50–350 mg/L

U(VI) is compared with different adsorbents in the literature. The fundamental characteristics of Langmuir model can be described as a dimensionless constant, i.e., separation factor (R_L) [25], expressed as:

$$R_L = 1/(1 + bC_0). \tag{5}$$

The inset of Fig. 6a shows the calculated R_L versus C_0. The R_L values are between 0 and 1, indicating that the

adsorption process is mainly process and therefore UHMWPEF-AO are suitable adsorbent.

3.4 Effect of temperature and thermodynamic studies

The adsorption of U(VI) on UHMWPEF-AO as a function of temperature was investigated by experiments at 295, 308, 318 and 333 K. As shown in Fig. 7, the amounts of U(VI) absorbed increased gradually with temperature, suggesting that U(VI) adsorption was endothermic and higher temperature is more favorable for the adsorption. Relative thermodynamic parameters were calculated by Eqs. (6)–(8):

$$k_d = q_e/C_e, \tag{6}$$

$$\ln k_d = \Delta S/R - \Delta H/(RT), \tag{7}$$

$$\Delta G = -RT\ln k_d, \tag{8}$$

where k_d (mL/g) is distribution coefficient; $R = 8.314$ J/mol/K is the gas constant; and ΔS (J/mol/K), ΔH (kJ/mol) and ΔG (kJ/mol) are changes in entropy, enthalpy and Gibbs free energy, respectively. The ΔS and ΔH can be calculated from the intercept and slope of ln k_d versus $1/T$ (see the inset of Fig. 7). The calculated ΔS, ΔH and ΔG are listed in Table 4. The positive value of ΔH verified the endothermic characteristic of the U(VI) absorption, while the positive value of ΔS exhibited the affinity of UHMWPEF-AO toward U(VI) under the experimental conditions and an increase in randomness between UHMWPEF-AO and the aqueous solution during the adsorption process. The negative values of ΔG show this process is the spontaneous. Moreover, the decreasing ΔG values indicate that the process is more effective at higher temperature [27]. Thermodynamic studies suggest
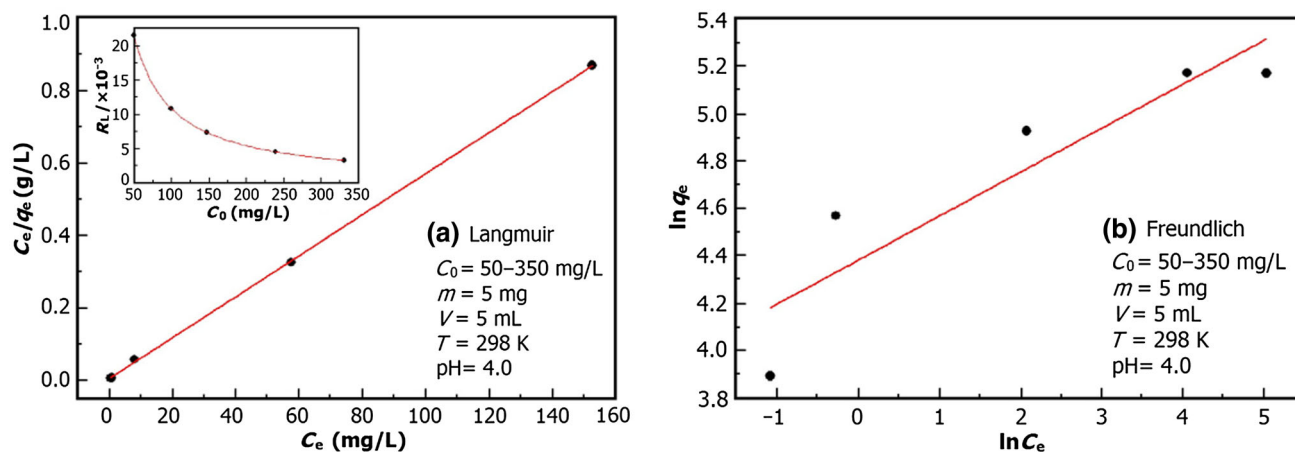
Fig. 6 (Color online) Langmuir (**a**) and Freundlich (**b**) plots for the adsorption of U(VI) by UHMWPEF-AO

Table 2 Isotherm parameters of U(VI) adsorption on UHMWPEF-AO

Isotherm model	Parameters	Value
Langmuir	q_m	176.99
	b	0.9142
	R^2	0.9998
Freundlich	n	5.7827
	k	79.8340
	R^2	0.7831

Table 3 Adsorption of U(VI) by various adsorbents

Adsorbents	T (K)	pH	q_m (mg/g)	Refs.
Fe_3O_4@PAM	293	5.0	220.94	[11]
CMPEI/CMK-3	293	4.0	151.5	[14]
CCTS	298	3.0	72.46	[17]
AO-g-MWCNT	298	4.5	145	[19]
HTC-COOH	308.15	6.0	205.8	[26]
UHMWPEF-AO	298	4.0	176.99	This work

the potential feasibility of UHMWPEF-AO as an adsorbent for U(VI).

3.5 Characterization of sample

FT-IR spectra of UHMWPEF-AO and U(VI)-loaded UHMWPEF-AO are shown in Fig. 8. In the UHMWPEF-AO spectrum, the broad peak at 3200–3400 cm^{-1} is relevant to –OH groups of amidoxime groups and water absorbed by physical adsorption during preservation. The peaks at 2921 and 2848 cm^{-1} correspond to antisymmetric and symmetric stretching vibrations of $–CH_2^-$, respectively [28]. The peaks at 1655 and 939 cm^{-1} are ascribed to –C = N- and –N–O- groups of amidoxime groups, separately [29]. In the spectrum of U(VI)-loaded UHMWPEF-AO, a new peak arises at 839 cm^{-1} corresponding to vibration of linear O = U = O [21], demonstrating that U(VI) was clearly adsorbed by complexing with amidoxime groups in UHMWPEF-AO.

U(VI)-loaded UHMWPEF-AO were removed from solutions after adsorption experiments ($C_0 \approx 100$ mg/L, $m = 5$ mg, $V = 5$ mL, pH = 4.0). The outer edge of the single fiber was selected through SEM and cut by FIB to form a cylinder about 12 μm in diameter and 12 μm deep. For Nano-CT experiments, X-ray energy was 8 keV and exposure time of single 2D image was 60 s. After 181 2D images were obtained with sample rotating from −90° to 90° at a constant velocity, the corresponding 3D tomography images were reconstructed. We used the Avizo Fire software 8.0 to analyze 3D tomography images. As shown in Fig. 9, U(VI) were absorbed along the outer edge of the single fiber. This was due to the surface complexation between amidoxime groups in UHMWPEF-AO and U(VI), consistent with results of kinetic studies and FT-IR spectra.

3.6 Sintering of the U(VI) loaded UHMWPEF-AO

U(VI)-loaded UHMWPEF-AO collected after adsorption were sintered at 1200 °C in an air atmosphere for 12 h. The morphology of powder obtained after sintering is shown in Fig. 10. Microparticles formed along the initial U(VI)-loaded UHMWPEF-AO and the angular microparticles had oval-like shape and smooth surface. The XRD pattern of the powder diffraction peaks at 14.9°, 21.3°, 25.8°, 26.4°, 33.7°, 43.4°, 46.2°, 51.6° and 73.7° ascribed to U_3O_8 (PDF#31-1424) and peaks at 27.9°, 30.4° and 33.7° assigned to U_2O_5(PDF#24-1362) is shown in Fig. 11.
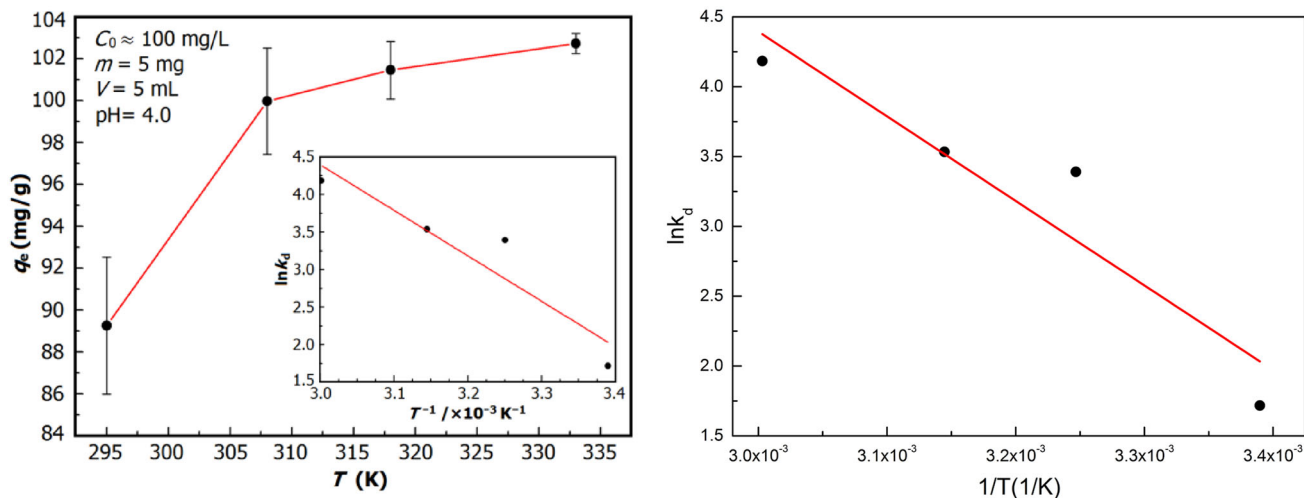
Fig. 7 (Color online) Effect of temperature on adsorption of U(VI)

Table 4 Thermodynamics parameters of U(VI) adsorption on UHMWPEF-AO

C_0 (mg/L)	ΔH (kJ/mol)	ΔS (J/mol/K)	ΔG (kJ/mol)			
			295 K	308 K	318 K	333 K
≈ 100	50.35	187.59	-4.21	-8.68	-9.34	-11.58
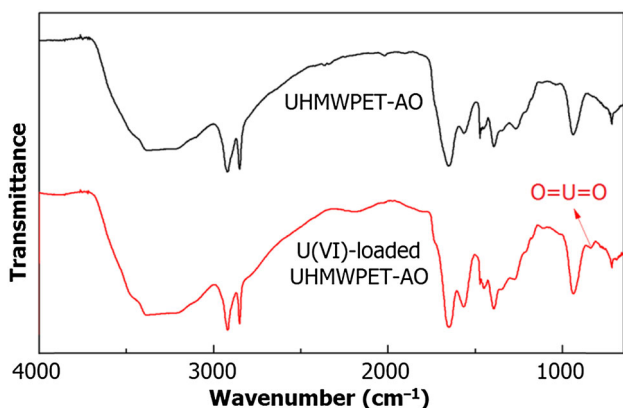
Fig. 8 (Color online) FT-IR spectra of UHMWPEF-AO and U(VI)-loaded UHMWPEF-AO

This result indicated that the powders were a mixture of uranium oxides.

Fig. 9 (Color online) 3D restructured structure of U(VI)-loaded UHMWPEF-AO

4 Conclusion

Amidoxime-functionalized ultra-high molecular weight polyethylene fibers were successfully applied for U(VI) recovery in aqueous solution as a simple and economical absorbing material. The pH value plays a critical role in the adsorption process. Kinetic and isotherm studies showed that the adsorption process met pseudo-second-order and Langmuir model. Moreover, experimental and calculated maximum adsorption capacity was 176.12 and 176.99 mg/g, respectively. Thermodynamic data proved that the adsorption of U(VI) on UHMWPEF-AO was endothermic and spontaneous. In addition, the structure of U(VI)-loaded UHMWPEF-AO was well characterized by FT-IR and CT, confirming that U(VI) in aqueous solutions were combined with UHMWPEF-AO. Importantly, the absorbed U(VI) can be easily recycled by sintering U(VI) loaded UHMWPEF-AO. Taken together, these evidences showed
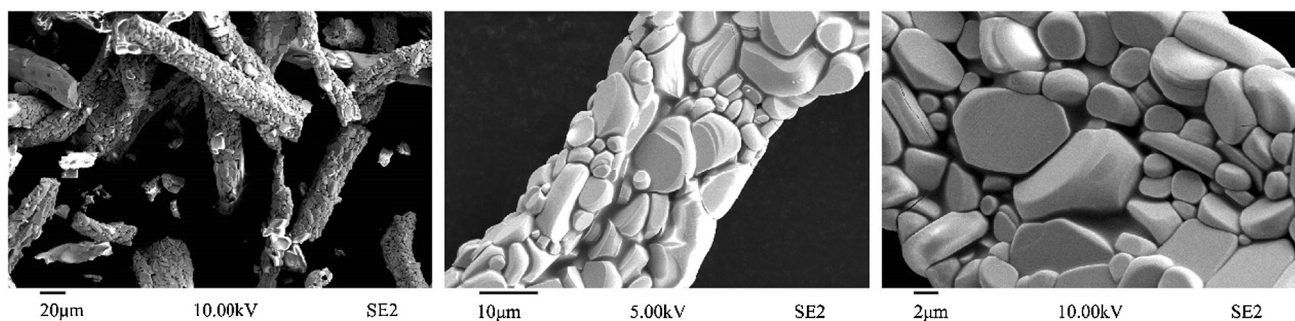
Fig. 10 SEM morphology of sintered U(VI)-loaded UHMWPEF-AO powder
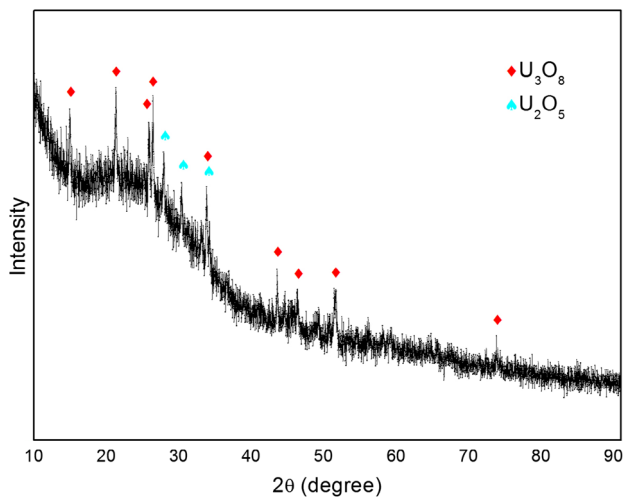
Fig. 11 (Color online) XRD pattern of sintered U(VI)-loaded UHMWPEF-AO powder

that UHMWPEF-AO serve as a probable candidate as an absorbent for removing U(VI) from aqueous solutions.

References

1. J.L. Liao, W. Wen, B. Li et al., Interaction between uranium and humic acid (II): complexation, precipitation and migration behavior of U(VI) in the presence of humic substances. Nucl. Sci. Tech. **24**, 030301-1–030301-9 (2013). doi:10.13538/j.1001-8042/nst.2013.03.010

2. World Health Organization, Guidelines for Drinking Water Quality. 2nd ed, Addendum to vol. 2. Health Criteria and other supporting information. (1996). http://www.who.int/water_sanitation_health/dwq/gdwq2v1/en/index1.html

3. World Health Organization, Guidelines for Drinking Water Quality. 3rd ed. (2003). http://www.who.int/water_sanitation_health/dwq/gdwq3rev/en/

4. T.P. Rao, P. Metilda, J.M. Gladis, Preconcentration techniques for uranium(VI) and thorium(IV) prior to analytical determination—an overview. Talanta **68**, 1047–1064 (2006). doi:10.1016/j.talanta.2005.07.021

5. O. Hazer, S. Kartal, Use of amidoximated hydrogel for removal and recovery of U(VI) ion from water samples. Talanta **82**, 1974–1979 (2010). doi:10.1016/j.talanta.2010.08.023

6. X.Q. Liu, Y.Y. Yang, J.L. Liao et al., efficient removal of uranium from mice by a novel compound of fullerence multimacrocyclic polyamine derivatives. Nucl. Sci. Tech. **26**, 040302-1–040302-8 (2015). doi:10.13538/j.1001-8042/nst.26.040302

7. A.P. Gilman, D.C. Villencuve, V.E. Seccours et al., Uranyl nitrate: 28-day and 91-day toxicity studies in the Sprague–Dawley rat. Toxicol. Sci. **41**, 117–128 (1998). doi:10.1016/toxs.1997.2367

8. H. Sodaye, S. Nisan, C. Poletiko et al., Extraction of uranium from the concentrated brine rejected by integrated nuclear desalination plants. Desalination **235**, 9–32 (2009). doi:10.1016/j.desal.2008.02.005

9. L.C. Tan, J. Wang, Q. Liu et al., Facile preparation of oxine functionalized magnetic Fe_3O_4 particles for enhanced uranium(VI) adsorption. Colloids Surf. A Physicochem. Eng. Asp. **466**, 85–91 (2015). doi:10.1016/j.colsurfa.2014.11.020

10. P.D. Bhalara, D. Punetha, K. Balasubramanian, A review of potential remediation techniques for uranium(VI) ion retrieval from contaminated aqueous environment. JECE **2**, 1621–1634 (2014). doi:10.1016/j.jece.2014.06.007

11. W.C. Song, M.C. Liu, R. Hu et al., Water-soluble polyacrylamide coated-Fe3O4 magnetic composites for high-efficient enrichment of U(VI) from radioactive wastewater. Chem. Eng. J. **246**, 268–276 (2014). doi:10.1016/j.cej.2014.02.101

12. H. Wang, X.Z. Shao, Q. Tian et al., Synthesis of TBP-coated magnetic Pst-DVB particles for uranium separation. Nucl. Sci. Tech **25**, 030301-1–030301-5 (2014). doi:10.13538/j.1001-8042/nst.25.030301

13. S.X. Duan, X. Liu, Y.N. Wang et al., Highly efficient entrapment of U(VI) by using porous magnetic $Ni_{0.6}Fe_{2.4}O_{0.4}$ micro-particles as the adsorbent. J. Taiwan Inst. Chem. Eng. **65**, 1–9 (2016). doi:10.1016/j.jtice.2016.05.041

14. Y.G. Zhao, J.X. Li, S.W. Zhang et al., Amidoxime-functionalized magnetic mesoporous silica for selective sorption of U(VI). RSC Adv. **4**, 32710–32717 (2014). doi:10.1039/c4ra05128a

15. Y.S. Zhao, C.X. Liu, M. Feng et al., Solid phase extraction of uranium(VI) onto benzoylthiourea-anchored activated carbon. J. Hazard. Mater. **176**, 119–124 (2010). doi:10.1016/j.jhazmat.2009.11.005

16. Y.J. Jung, S. Kim, S.J. Park et al., Preparation of functionalized nanoporous carbons for uranium loading. Colloids Surf. A Physicochem. Eng. Aspects. **313–314**, 292–295 (2008). doi:10.1016/j.colsurfa.2007.04.112

17. D.D. Shao, G.S. Hou, J.X. Li et al., PANI/GO as a super adsorbent for the selective adsorption of uranium(VI). Chem. Eng. J. **255**, 604–612 (2014). doi:10.1016/j.cej.2014.06.063

18. Y.G. Zhao, J.X. Li, L.P. Zhao et al., Synthesis of amidoxime-functionalized Fe$_3$O$_4$@SiO$_2$ core-shell magnetic microspheres for highly efficient sorption of U(VI). Chem. Eng. J. **235**, 275–283 (2014). doi:10.1016/j.cej.2013.09.034

19. Y.G. Zhao, X.X. Wang, J.X. Li et al., Amidoxime functionalization of mesoporous silica and its high removal of U(VI). Polym. Chem. **6**, 5376–5384 (2015). doi:10.1039/c5py00540j

20. Z. Xing, J.T. Hu, M.H. Wang et al., Properties and evaluation of amidoxime-based UHMWPE fibrous adsorbent for extraction of uranium from seawater. Sci. China Chem. **56**, 1504–1509 (2013). doi:10.1007/s11426-013-5002-x

21. G.H. Wang, J.S. Liu, X.G. Wang et al., Adsorption of uranium (VI) from aqueous solution onto cross-linked chitosan. J. Hazard. Mater. **168**, 1053–1058 (2009). doi:10.1016/j.jhazmat.2009.02.157

22. A.Y. Zhang, T. Asalura, G. Uchiyama, The adsorption mechanism of uranium (VI) from seawater on a macroporous fibrous polymeric adsorbent containing amidoxime chelating functional group. React. Funct. Polym. **57**, 67–76 (2003). doi:10.1016/j.reactfunctpolym.2003.07.005

23. Y. Wang, Z.X. Gu, J.J. Yang et al., Amidoxime-grafted multi-walled carbon nanotubes by plasma techniques for efficient removal of uranium(VI). Appl. Surf. Sci. **320**, 10–20 (2014). doi:10.1016/j.apsusc.2014.08.182

24. K.Y. Foo, B.H. Hameed, Insights into the modeling of adsorption isotherms systems. Chem. Eng. J. **156**, 2–10 (2010). doi:10.1016/j.cej.2009.09.013

25. H. Wang, L.J. Ma, K.C. Cao et al., Selective solid-phase extraction of uranium by salicylideneimine-functionalized hydrothermal carbon. J. Hazard. Mater. **229–230**, 321–330 (2012). doi:10.1016/j.jhazmat.2012.06.004

26. Y.H. Liu, Y.Q. Wang, ZhB Zhang et al., Removal of uranium from aqueous solution by a low cost and high-efficient adsorbent. Appl. Surf. Sci. **273**, 68–74 (2013). doi:10.1016/j.apsusc.2013.01.182

27. S.P. Chen, J.X. Hong, H.X. Yang et al., Adsorption of uranium(VI) from aqueous solution using a novel graphene oxide-activated carbon felt composite. J. Environ. Radioact. **126**, 253–258 (2013). doi:10.1016/j.jenvrad.2013.09.002

28. X.Y. Liu, H.Z. Liu, H.J. Ma et al., Adsorption of the Uranyl Ions on an amidoxime-based polyethylene nonwoven fabric prepared by preirradiation-induced emulsion graft polymerization. Ind. Eng. Chem. Res. **51**, 15089–15095 (2012). doi:10.1021/ie301965g

29. Y.G. Zhao, J.X. Li, S.W. Zhang et al., Efficient enrichment of uranium(VI) on amidoximated magnetite/graphene oxide composites. RSC Adv. **3**, 18952–18959 (2013). doi:10.1039/c3ra42236d